ST. ANTHONY FALLS HYDRAULIC LABORATORY
UNIVERSITY OF MINNESOTA

Project Report No. 32

# MODEL STUDIES OF A WATER TUNNEL WITH AN AIR-BUBBLE RESORBER

*Supplement I to Project Report No. 29*

## A Diverging Closed-Jet Test Section for a Water Tunnel

*Submitted by*
LORENZ G. STRAUB
Director

*Prepared by*
REUBEN M. OLSON


June, 1952

Prepared for the
DAVID TAYLOR MODEL BASIN
Department of the Navy
Washington, D.C.

Bureau of Ships Contract N600s-s-11459

# PREFACE

Contract N600s-s-11459 between the University of Minnesota, St. Anthony Falls Hydraulic Laboratory and the Department of the Navy, Bureau of Ships, David Taylor Model Basin provided for model studies of a proposed design for a 36-in. water tunnel with an air-bubble resorber. This report covers studies made of a diverging closed-jet test section for this tunnel. The work was begun under the above contract and was completed under an extension to this contract.

The experimental program was carried out under the general direction of Dr. Lorenz G. Straub, Director of the St. Anthony Falls Hydraulic Laboratory. The studies were conducted by R. M. Olson, with the assistance of T. Timar prior to January 1, 1952. The analysis of Appendix B is based on an unpublished paper by J. S. Holdhusen. Preparation of the manuscript was done by L. A. Johnson, Leona S. Wray, J. J. Casey, and M. Manohar. Mr. W. F. Brownell represented the David Taylor Model Basin in the technical aspects of the project.

# CONTENTS

# LIST OF ILLUSTRATIONS

## ABSTRACT

The original closed-jet test section designed for use in a 36-in. water tunnel with an air-bubble resorber was cylindrical and 2.18 diameters long. It was followed by a parabolic transition, 0.5 diameter long, to the $7^{\circ}$ diffuser cone. The effect of a diverging test section with a longer diffuser transition in decreasing the pressure gradients and, as a result, lowering the cavitation indices attainable is discussed in this report.

Tests on a one-sixth scale model and analyses indicate that a test section diverging at a total angle of about $0^{\circ}$ 9.6' would be expected to have an essentially constant core pressure throughout the length of the test section. This divergence angle followed by a nearly 1-diameter transition should result in a test section which can be operated at cavitation indices as low as 0.025 or 0.030 at velocities of 84.5 fps.

# MODEL STUDIES OF A WATER TUNNEL WITH AN AIR-BUBBLE RESORBER

## A DIVERGING CLOSED-JET TEST SECTION FOR A WATER TUNNEL

### I. INTRODUCTION

It is desirable in the test section of a closed-jet water tunnel to have a uniform flow field and to be able to attain as low a cavitation index as possible. The customary closed-jet test section is cylindrical in shape and is usually preceded by a nozzle or contraction and is followed by a diffuser for recovering the jet energy. A transition is placed between the test section and the diffuser to reduce the wall pressure gradients which would enhance separation. This arrangement results in radial pressure gradients most noticeable in the diffuser transition region, which would be expected from potential theory. In addition the boundary layer, which increases in the direction of flow, is a region of retarded velocity and thus, from continuity principles, the core velocity in the test section must increase in the direction of flow. This increase in the core velocity is accompanied by a decrease in core pressure, since there is no appreciable energy loss in the core flow. The minimum cavitation index attainable at the upstream axis of the test section is determined by the effectiveness of the diffuser transition in retarding adverse pressure gradients along the walls, by the longitudinal pressure drop either along the axis or the wall, by the radial variations in piezometric pressure, and by the static head difference between the top of the test section and the axis. These are based on cavitation originating at the top of the diffuser transition, which is usually the point of minimum pressure in the tunnel circuit.

Previous tests in the closed-jet test section of a 6-in. model of a 36-in. water tunnel indicated an axial pressure drop of about 2 per cent of a velocity head (based on mean velocity in the bare test section), radial variations as high as 5 per cent of a velocity head, and a minimum cavitation index of about 0.065 at the upstream axis of the test section at a velocity of 84.5 fps [1].* The length of the diffuser transition was 0.5 test-section diameter. It seemed likely that a test section which diverged slightly to compensate for the boundary layer thickness could have an essentially constant

---

*Numbers in brackets refer to references listed on page 11.

core pressure. If the diffuser transition were lengthened, the sharp drop in wall pressure in the transition region would be decreased. The expected result would be a more uniform flow field and a lower minimum cavitation index for the tunnel.

Two diverging test sections were constructed and tested. The total angle of divergence in each was $0^{\circ}$ 11.6'. The first had only a diffuser transition, the taper beginning abruptly at the end of the cylindrical end of the contraction cone. The joint between the contraction and test section was at this point, and it was thought that the effect of the divergence angle and longer transition could be determined without machining a transition into the contraction cone piece. The second test section was the same as the first except it had both a contraction and a diffuser transition, with the joint between the contraction cone and the test-section piece upstream of the contraction transition. These changes were made because it was not known whether some erratic results from the first assembly were due to the abrupt taper or to the boundary joint which was located at the beginning of the taper.

The present tests involved the determination of the pressure gradients in the test-section region of the model tunnel and the expected cavitation characteristics of the 36-in. prototype tunnel. A method for designing a constant-pressure test section, verified by the model tests, is given in order to determine the optimum design of the prototype test section.

## II. THEORETICAL CONSIDERATIONS

Analytical methods for determining the axial pressure change in a cylindrical or diverging test section customarily neglect the effects of curvilinear flow in the entrance and exit regions. In a short test section, these effects are measurable well into the test section itself. Nevertheless, the methods are quite useful in establishing trends and the order of magnitude of effects of changes in the design variables. They also serve as a basis for interpreting the results of model tests and for predicting prototype performance.

In order to design a constant-pressure test section, the amount of flow which is retarded in the boundary layer must be known. This is done to a first approximation in Appendix B by using the theory of boundary-layer growth on a flat plate. The resulting equation for the axial pressure coefficient is

$$C_p = \frac{(P_2 - P_o)/w}{V_o^2/2g} = \left[\frac{R_o^2}{R_o\,(R_o - 2\delta_o)}\right]^2 - \left[\frac{R_o^2}{R_2\,(R_2 - 2\delta_2)}\right]^2 \qquad (1)$$

where $P_2$ is the pressure intensity at the downstream end of the test section,

$P_o$ is the pressure intensity at the upstream end of the test section,

$w$ is the specific weight of the fluid,

$V_o$ is the mean velocity at the upstream end of the diverging test section,

$R_o$ and $R_2$ are the upstream and downstream test-section radii, respectively, and

$\delta_o$ and $\delta_2$ are equivalent to the displacement thickness for two-dimensional flow at the upstream and downstream ends of the test section, respectively; they are functions of the Reynolds number as indicated in Appendix B.

The pressure coefficient as used here is restricted to the dimensionless pressure change from the upstream to the downstream end of the test section. With a zero pressure gradient, the boundary-layer growth should approximate that on a flat plate. For a decreasing pressure, it should be less, and thus the decrease in pressure would be less than that for a flat plate. The converse is true for an increasing pressure. In both instances the effect is to make the pressure coefficient smaller than that for a flat plate. A reduction of 10 per cent was used in the present analysis. This figure was obtained from an analysis of the pressure gradient resulting from boundary-layer development in a cylindrical smooth pipe when the pressure coefficient was -0.01 per diameter of length [2].

The results of the computations are shown in Fig. 1. The downstream radius required for a constant-pressure core flow for various Reynolds numbers is given. This is based on an upstream radius of 1.500 ft. Also shown are the expected pressure coefficients for other than optimum designs. Figure 2 shows the expected core pressure coefficient for various values of downstream radius for the model at a Reynolds number corresponding to a velocity of 48 fps at a water temperature of 74° F. These were the conditions for most of the model tests.

## III. MODEL STUDIES

The water tunnel used in earlier tests [1] was also used in the current studies. Two diverging test sections were tested with this tunnel.

In the first, the former cylindrical test section was modified to obtain a diverging test section followed by a longer diffuser transition than was previously used. In order to minimize the fabrication changes, the tapered portion began abruptly at the end of the contraction piece; a transition would have required machining of the contraction. However, test results later indicated this to be desirable. The second test section assembly was similar to the first except that it extended physically about halfway into the contraction and had a 0.5-diameter transition at the beginning of the taper. Results of tests on both assemblies are included in this report.

A. Diverging Closed-Jet Test Section with Diffuser Transition

A tentative design for a diverging test section was specified in reference [3]. It consisted of a taper of 0.00170 in. per in. ($0^\circ$ 5.8' half angle) for 72.36 in. (2.01 diameters) followed by a parabolic transition 34.98 in. long (0.972 diameter). In order that the design of the remainder of the tunnel would not be affected by changes in the design of the test section, it was specified that the end points of the original test-section assembly (Fig. 3 of reference [4]) were to remain fixed. These end points were in the downstream end of the contraction and the upstream portion of the diffuser.

The geometrical model of the tentative prototype design is shown in Fig. 3. The taper began at the joint between the aluminum contraction core and the acrylic resin test-section piece, and it is possible that there were slight discontinuities of perhaps 0.002 or 0.003 in. at the joint.

Wall pressures, axial pressures, and differences between the axis and wall pressures were measured. The axial pressures were measured with an extension of the contraction dynamometer shaft housing as described in reference [1]. Wall pressure variations are shown in Fig. 4. From the data plotted in this figure, it is seen that there was considerable scatter in the measurements in the upstream portion of the test section (additional data obtained near $x/D_o = 0$ are not shown). For this reason the graph was plotted with respect to no particular reference; the shape of the curve in the diffuser transition region was of primary interest. The sharp drop in pressure indicated in Fig. 36 of reference [1] was essentially eliminated by the longer transition.

A point of low pressure near the beginning of the test section was indicated by the wall pressure measurements and was verified by cavitation

tests. Evidence of secondary cavitation inception near the beginning of the test section is shown in Fig. 5. It was not known whether this condition was due to the abrupt taper or to the joint in the tunnel assembly.

Axial pressure variations are shown in Fig. 6. The curve shapes are very similar to those previously obtained for a cylindrical test section (Fig. 37 of reference [1]). The present curves of Fig. 6, however, indicate an essentially constant-pressure core. The effects of curvilinear flow in the contraction probably account for the slight rise in pressure at the upstream end of the test section.

Measured pressure differences between the axis and the walls of the test section are shown in Fig. 7. The curve is of most interest in the transition region, where the difference of about 2.5 per cent of the velocity head is considerably less than the 5.5 per cent value measured with the cylindrical test section with a shorter transition. The scatter in the data for values of $x/D_o$ between 0 and 1.0 reflect the erratic wall pressures indicated in Fig. 4.

As a result of the erratic wall pressures near the upstream end of the test section and the occurrence of cavitation there, it was decided to fabricate a new test-section piece which would extend upstream into the contraction and which would have a transition at the beginning of the taper extending 0.25 diameter both upstream and downstream of the beginning of the test section.

B. Diverging Closed-Jet Test Section with Both Contraction and Diffuser Transitions

The second test section is shown in Figs. 8 and 9. It was made of an acrylic resin plastic which included the downstream portion of the contraction, the contraction transition, the test section, the diffuser transition, and a part of the $7^\circ$ diffuser. The upstream end of this plastic piece extended 10 in. further upstream than formerly; this required the removal of the downstream 10 in. of the aluminum contraction casting. The profile in the portion of the contraction casting which was removed had some slight irregularities (Fig. 22 of reference [1]), and the new contour which was machined into the new plastic piece was modeled after the recommended prototype profile (Table II of reference [1]). Slight adjustments were made between x = -5 and -10 in. in order to avoid a discontinuity at the new joint. The coordinates for the plastic section used in the model are given in Table I, page 27.

Wall pressures measured at numerous pairs of diametrically opposite piezometer taps are shown in Fig. 10. Only one set of recorded data obtained at a velocity of 49 fps are shown. Some scatter in the data is indicated; however, all points were reproducible within 0.1 or 0.2 per cent of a velocity head at different rotational orientations of the test section and at different times. This indicates that the data are reliable and that no axial nonsymmetry or skewness existed in the tunnel in the test-section region. Data obtained at 30 fps agreed with all points plotted in Fig. 10 between $x/D_o = -0.5$ and +2.4 within 0.2 per cent of a velocity head. It is not believed that the scatter is due to variations or errors introduced by piezometer tap geometry, since similar tap geometries were used for the axial measurements and little scatter was noticed (Figs. 6 and 11 and Figs. 34 and 37 of reference [1]). The scatter is probably due to slight undulations in the wall. The model test section was machined using a handmade template with a manual template-follower arrangement. Although the dimensions were within the tolerances specified, some waviness probably existed. The pressures shown in Fig. 10 are believed to represent actual wall pressures.

Comparison of the curve faired through the plotted points with that for the cylindrical test section with a shorter diffuser transition indicates that considerable improvement was made. A dip which might be indicated by the three low points near $x/D_o = 2.2$ was not indicated in the curves of Fig. 4 and thus were not given full weight. The curves of Fig. 4 were obtained from a test section with identically designed diffuser transition regions. The absence of a dominating sharp pressure drop was also indicated in cavitation studies.

Axial pressure variations are shown in Fig. 11. An essentially constant core pressure is indicated. The computed coefficient (Fig. 2) was about -0.3 per cent of a velocity head, and the agreement between the curves and this value is considered satisfactory if allowance is made for the effect of the diffuser transition upstream into the test section. Similar agreement exists between the extrapolated value of -2.7 per cent for a cylindrical test section from Fig. 2 and the measured axial pressure if end effects are taken into account (Fig. 37 of reference [1]).

The radial differences in piezometric pressure between the axis and the wall are shown in Fig. 12. The data are most useful in the diffuser transition region in determining the minimum cavitation index for the tunnel. The scatter near the upstream end of the test section again reflects the scatter in wall pressures shown in Fig. 10.

The cavitation characteristics of the model test section were not only indicated by the pressure measurements but were also studied directly. In these tests the measured pressure at the inception of cavitation was never as low as vapor pressure but was a minimum of about 1 ft of water above vapor pressure. Cavitation inception was apparently a function of some property of the water other than its vapor pressure, and the cavitation indices will, then, be based on this critical pressure rather than vapor pressure. This will permit a comparison of the cavitation characteristics of the boundary shapes with no dependence on the cavitating properties of the fluid.

Various degrees of cavitation in the model test section are shown in Fig. 13. The photographs were taken at an exposure time of about 20 microseconds. The cavitation indices indicated apply to the axis at the upstream end of the test section and are based on critical pressure at cavitation inception rather than vapor pressure. The actual test-section portion of the plastic piece is indicated by the white line. Figure 13a indicates not only that cavitation had not begun, but also that the tunnel water was free of entrained bubbles. In Fig. 13b, cavitation just began at the top of the diffuser transition. The test-section pressure was lowered and the velocity increased in each successive picture in the series, and Figs. 13b to 13f show increasing severity of cavitation. This test-section pressure was the result of maintaining the pressure at the upstream end of the contraction slightly above atmospheric, and using the pressure drop through the contraction at various velocities to obtain desired pressures in the test section. In the photographs, a line drawn along the upstream limit of cavitation bubbles should be a line of essentially constant absolute pressure (the present analysis applies to wall pressures only). In Fig. 13c, for example, bubbles began to appear at about the centerline level in the diffuser transition region, which is 0.25 ft or $0.25/34.4 = 0.007$ velocity heads higher pressure than at the top of the diffuser transition where cavitation first began. Bubbles also appear near the top of the test section near the upstream end of the test section, and thus the pressure there would also be about 0.007 velocity heads greater than at the top of the diffuser transition. This agrees quite well with the curve of Fig. 10. The photographs of Fig. 13d to 13f indicate that a reasonably constant-pressure test section was designed. Of course, the presence of test bodies would alter the conditions and would provide a factor of safety in ensuring that tunnel cavitation inception would not occur in the upstream end of the test section. This might not be true for a bare tunnel if the divergence angle were too large.

## IV. ESTIMATED PROTOTYPE PERFORMANCE

The pressure gradient in the diverging prototype test section will, of course, be dependent on the downstream radius and the operating Reynolds number. It is indicated in Fig. 1 that the tentative downstream radius of 1.51025 ft (diameter of 36.246 in.) will have a zero axial pressure gradient at a Reynolds number of $4 \times 10^6$, but will have an increasing core pressure of about 0.5 per cent of a velocity head under normal operating conditions. This is an over-correction, but should result in a lower minimum cavitation index. If the primary objective is a constant-pressure core flow in the bare test section, with some sacrifice in achieving the lowest possible cavitation index, a downstream radius of about 1.5085 ft would be more desirable for the usual range of test velocities. Five possible test-section profiles are shown in Fig. 14. These profiles are for downstream radii of 1.508 to 1.51025 ft, giving a zero pressure gradient at Reynolds numbers (based on test-section diameter) from $4 \times 10^6$ to $2.5 \times 10^7$ (Fig. 1). The test-section length is the same for all these profiles, and the length of the diffuser transition ranges between 33.86 and 34.98 inches. This variation is negligible, and thus the model measurements of wall pressures should be representative of those expected in the prototype for any degree of test-section divergence included in Fig. 14. No changes have been made in the overall length, relative position of the contraction or diffuser, or in the end diameters from those originally specified for the cylindrical test section (Fig. 3 of reference [4]).

The minimum cavitation index along the axis of the test section will be a function of the wall, axis, and radial pressure variations. If the prototype test section diverges such that it has an axial pressure variation similar to that of the model (Fig. 11), the estimated cavitation indices for various velocities are as shown in Fig. 15. This axial pressure condition will exist if the downstream radius is about 1.508 ft. The upper portion of each band in Fig. 15 is based on some measured points of Figs. 10, 11, and 12, while the lower portion is based on the curves of Figs. 10 to 12. Vapor pressure (or some critical pressure, if the cavitation index is so defined) was assumed to exist at the top of the diffuser transition (at $x/D_o = 2.08$ and 2.17, the location of minimum pressure in the diffuser transition region from Fig. 10) and the dimensionless pressure difference between this point

and the upstream centerline of the test section was obtained from Figs. 10 to 12. A number of paths along the wall, radially to the axis, and then upstream along the axis to the beginning of the test section were used, the crossing to the axis being made at values of $x/D_o$ = 2.25, 2.17, 2.08, 2.0, 1.58 for the measured points. In addition to these, crossings were made at $x/D_o$ = 1.25 and 1.00 when using the curves. In the first instance (upper portion of the curves of Fig. 15) the minimum wall pressure was assumed to be that given by the lower points at $x/D_o$ = 2.1 in Fig. 10, and in the second (lower portion of the curves of Fig. 15) by the lowest part of the curve.

The minimum cavitation indices at the upstream end of the axis of the test section are, then, given by

$$\sigma_{min} = 1.6 + \frac{1.5}{V_o^2/2g} \tag{2}$$

based on the measured points, and

$$\sigma_{min} = 1.1 + \frac{1.5}{V_o^2/2g} \tag{3}$$

based on the curves of Figs. 10 to 12. The 1.1 and 1.6 figures are the mean dimensionless pressure differences mentioned above and are the average of five and seven individual determinations, respectively. All the above values obtained from Figs. 10 to 12 were within 0.2 of a velocity head of the 1.1 and 1.6 figures.

The minimum cavitation index at the centerline of the pump intake will be reduced by 0.051 - 0.011 = 0.04 (Eq. (15) of reference [1] and Eq. (3) of this report) divided by the tunnel loss coefficient of about 0.23 compared to that indicated in Fig. 79 of reference [1]. Thus curve A of Fig. 79, reference [1], will be lowered 0.16, a negligible amount.

Likewise, the minimum cavitation index at the axis of elbow I immediately following the main diffuser will be essentially the same as that given by Eq. (12) of reference [1], and the elbow should be free of cavitation. The tunnel losses in any case should not be noticeably affected by changing from a cylindrical to a diverging test section.

## V. CONCLUSIONS

As a result of the analysis for the design of a constant-pressure closed-jet test section and the model tests on a diverging test section, it is indicated that for the prototype diverging test section without test bodies

1. An essentially constant core pressure may be attained with a diverging test section.

2. The use of a longer diffuser transition (1 diameter instead of 0.5 diameter, as was used with the cylindrical test section) essentially eliminated the sharp drop in wall pressure which was present with the shorter transition and also reduced the radial pressure variations in the transition region.

3. A curved transition from the end of the contraction to the diverging test section is desirable, with the physical joint in the tunnel assembly located upstream of this point.

4. A cavitation index of about 0.025 or 0.03 should be attainable in the bare test section. A value even lower than these could be achieved if the core pressure rises in the direction of flow. The pump and vaned elbows are expected to be free of cavitation if operational limits are established by these values.

# REFERENCES

[1] Olson, R. M. Model Studies of a Water Tunnel with an Air-Bubble Resorber. University of Minnesota, St. Anthony Falls Hydraulic Laboratory Project Report No. 29, February, 1952.

[2] Holdhusen, J. S. "The Turbulent Boundary Layer in the Inlet Region of Smooth Pipes." Unpublished Ph.D. thesis, Library, University of Minnesota, February, 1952.

[3] Brownell, W. F., David Taylor Model Basin. Letter to Dr. L. G. Straub, St. Anthony Falls Hydraulic Laboratory, University of Minnesota, Minneapolis, Minnesota, November 27, 1951.

[4] Brownell, W. F. Functional Specifications of a 36-inch Variable Pressure Water Tunnel for the David Taylor Model Basin. Department of the Navy, David Taylor Model Basin File N8/2 - 1 (518:WFB:mmb), April, 1951.

[5] Water Tunnel Working Section Flow Studies. Pennsylvania State College, Ordnance Research Laboratory Report NOrd 7958-97, June 15, 1948.

[6] Landweber, L. Effect of Transverse Curvature on Frictional Resistance. Department of the Navy, David Taylor Model Basin Report 689, March, 1949.

# APPENDICES

# APPENDIX A

## LIST OF SYMBOLS

$C_f$ - Local coefficient of wall shear.

$C_p$ - Pressure coefficient.

$D_o$ - Test-section diameter at upstream end.

$D_2$ - Test-section diameter at downstream end.

$g$ - Acceleration of gravity.

$P$ - Pressure intensity in pounds per square foot absolute.

$P_{Axis}$ - Axial pressure intensity.

$P_c$ - Critical pressure intensity at cavitation inception.

$P_{vp}$ - Vapor pressure of the fluid.

$P_{Wall}$ - Wall pressure intensity.

$P_x$ - Pressure intensity at some downstream point in the test section.

$P_o$ - Pressure intensity at upstream end of the test section.

$P_2$ - Pressure intensity at downstream end of the test section.

$R$ - Radius of test section.

$Re$ - Reynolds number.

$Re_X$ - Reynolds number based on $X$.

$R_o$ - Radius at upstream end of test section.

$R_1$ - Radius in contraction transition.

$R_2$ - Radius at downstream end of test section.

$R_3$ - Radius in diffuser transition.

$r$ - Radial distance from centerline to any point in the flow stream.

$V$ - Mean temporal longitudinal velocity.

$V_o$ - Mean bulk-flow velocity in a 6-in. diameter test section in the model or a 36-in. diameter test section in the prototype (bare test section without dynamometer shafts) in feet per second.

$V_{oc}$ - Core velocity at the beginning of the test section.

$V_{2c}$ - Core velocity at the end of the test section.

$w$ – Specific weight of fluid in pounds per cubic foot.

$X$ – Distance from leading edge of a flat plate.

$x$ – Distance downstream of beginning of test section.

$x_1$ – Distance downstream of beginning of contraction transition (at $x/D_o = -0.25$).

$x_3$ – Distance downstream of beginning of diffuser transition (at $x/D_o = 2.01$).

$Y$ – Disturbance thickness of the boundary layer in a circular conduit.

$Y'$ – Disturbance thickness of a two-dimensional boundary layer.

$y$ – Radial distance measured from the boundary wall.

$\Delta P$ – Change in pressure intensity.

$\delta$ – Linear measurement of the discharge which has been retarded in the conduit boundary layer.

$\delta'$ – Two-dimensional displacement thickness.

$\nu$ – Kinematic viscosity.

$\sigma_{min}$ – Minimum cavitation index at the upstream end of the test-section axis when cavitation occurs at some other point in the tunnel without test bodies or dynamometer shafts in place

$$\sigma = \frac{(P - P_c)/w}{V_o^2/2g} \quad \text{or} \quad \sigma = \frac{(P - P_{vp})/w}{V_o^2/2g} .$$

$\sigma_o$ – Cavitation index at the upstream end of the test-section axis.

# APPENDIX B

## DESIGN OF A CONSTANT-PRESSURE CLOSED-JET TEST SECTION*

When fluid flows in a conduit, the boundary shear causes the fluid to be retarded near the conduit walls. This retarded region increases in the direction of flow. If it is assumed that the velocity distribution at the entrance is uniform and that a turbulent boundary layer begins to develop there, the central core will have no normal velocity gradient for some distance along the conduit and thus the total energy of the core flow will remain constant. In order to maintain continuity the core velocity must increase, and thus the pressure drop can be computed if this velocity increase is known. It should be possible to design a conduit with an area increasing in the direction of flow in a manner such that the core velocity is constant. In order to do this, the amount of flow retarded in the boundary layer must be known. This can be done to a first approximation by using the theory of boundary-layer development on smooth, flat plates.

Consider a circular conduit which has an initial radius $R_o$ and a uniform velocity $V_o$ at the entrance. If at some downstream point the disturbance thickness is $Y$, continuity may be maintained with a constant core velocity if

$$\pi R_o^2 V_o = \pi (R - Y)^2 V_o + \int_{R-Y}^{R} 2\pi r V \, dr \tag{4}$$

where R is the varying radius of the conduit,
r is the radial distance from the axis, and
V is the mean temporal velocity at $r$.

Equation (4) may be written as

$$\frac{R}{R_o} = \frac{\delta}{R_o} + \sqrt{\left(\frac{\delta}{R_o}\right)^2 + 1} \tag{5}$$

where

$$\delta = \frac{1}{R} \int_{R-Y}^{R} \left(1 - \frac{V}{V_o}\right) r \, dr \tag{6}$$

---

*Digested from an unpublished paper by James S. Holdhusen and from reference [5]. Similar methods were used by Holdhusen for designing a diverging test section with a constant-pressure core and in reference [5] for determining the pressure coefficient for a cylindrical test section.

The quantity $\delta$ is a linear measurement of the amount of discharge that has been retarded in the boundary layer and is analogous to the two-dimensional displacement thickness

$$\delta' = \int_0^{Y'} \left(1 - \frac{V}{V_o}\right) dy \tag{7}$$

where y is measured radially from the flow boundary, and

Y' is the disturbance thickness of the two-dimensional boundary layer.

The effect of the concave transverse curvature of the conduit is expected to increase the disturbance thickness beyond that expected for a flat plate. On the basis of the calculations made in reference [6], this increase is estimated to be a maximum of 4 per cent in the present case, so that $Y/Y' = 1.04$.

If the velocity distribution in a boundary layer is assumed to be represented by

$$\frac{V}{V_o} = \left(\frac{y}{Y'}\right)^{1/7} \tag{8}$$

then substitution of this in Eq. (7) will show that

$$\delta' = \frac{Y'}{8} \tag{9}$$

and substitution in Eq. (6), with $y = R - r$, will show that

$$\delta = \frac{Y}{8} - \frac{Y^2}{30R} \tag{10}$$

Thus

$$\frac{\delta}{\delta'} = \frac{Y}{Y'}\left[1 - \frac{4Y}{15R}\right] \tag{11}$$

For a value of Y/R of 0.13 and estimating $Y/Y' = 1.04$, $\delta/\delta' = 1.004$. This means that there will be an average error of less than 1 per cent in $\delta$ if $\delta'$, as computed from two-dimensional boundary-layer theory, is used for $\delta$. This is probably better than the accuracy with which $\delta'$ can be computed.

From reference [5] the displacement thickness of a two-dimensional boundary layer is

$$\delta' = \frac{Y'}{K}\sqrt{\frac{C_f}{2}} \tag{12}$$

where K is a constant, approximately equal to 0.40, and

$C_f$ is the local coefficient of wall shear.

The disturbance thickness is

$$Y' = 0.40\ X\ \sqrt{C_f} \tag{13}$$

so that

$$\delta \simeq \delta' = \frac{X\ C_f}{\sqrt{2}} \tag{14}$$

The value of $C_f$ is given by

$$\frac{1}{\sqrt{C_f}} = 1.7 + 1.8\,\ell n\ (Re_X\ C_f) \tag{15}$$

In Eqs. (13) to (15), $\underline{X}$ is the distance from the leading edge of the flat plate or the entrance to the circular conduit (estimated to be 0.25 diameter upstream of the beginning of the test section for the present calculations), and $Re_X$ is the Reynolds number based on this length.

It should be emphasized that the analysis is valid for a section of a conduit which has an initial boundary layer as well as for one which does not have an initial boundary layer. Actually, the results are only moderately sensitive to variations of the order of 0.5 diameter in the hypothetical location of the beginning of the boundary layer.

Since there are no appreciable losses in the core flow, the axial or core pressure coefficient is obtained from the energy equation as

$$C_p = \frac{(P_2 - P_o)/w}{V_o^2/2g} = \frac{V_{oc}^2 - V_{2c}^2}{V_o^2} \tag{16}$$

where $V_{oc}$ and $V_{2c}$ are the core velocities at the upstream and downstream ends of the test section, respectively, and

$V_o$ is the mean upstream test-section velocity.

From the definition of $\delta$

$$V_{oc} = V_o \frac{R_o^2}{R_o (R_o - 2\delta_o)}$$

and

$$V_{2c} = V_o \frac{R_o^2}{R_2 (R_2 - 2\delta_2)}$$

so that

$$C_p = \left[\frac{R_o^2}{R_o (R_o - 2\delta_o)}\right]^2 - \left[\frac{R_o^2}{R_2 (R_2 - 2\delta_2)}\right]^2 \qquad (17)$$

For a zero pressure gradient, Eq. (17) becomes

$$R_2 = \delta_2 + \sqrt{\delta_2^2 + R_o (R_o - 2\delta_o)} \qquad (18)$$

In computing $\delta_o$ and $\delta_2$ from Eq. (14), $X_o/D_o$ was assumed to be 0.25 test-section diameter and $X_2/D_o$ was 2.01 test-section diameters greater than $X_o/D_o$.

The curve of Fig. 2 for the model was obtained from Eq. (17), and the curves of Fig. 1 were obtained from a family of similar curves for the prototype. Reference [2, pp. 41 to 45] indicates that the effect of a pressure gradient on the growth of a boundary layer in a circular conduit and the subsequent effect of altering this pressure gradient are such that a correction of about 20 per cent of $C_p$ if $C_p$ = 0.02 per diameter, 10 per cent if $C_p$ = 0.01 per diameter, and about 5 per cent if $C_p$ = 0.005 per diameter should be applied to decrease the pressure coefficient computed from Eq. (17). The line for Fig. 2 was corrected by a mean value of 10 per cent; the curve obtained by the more precise corrections departs from the line a negligible amount.

The model test sections which were tested and the prototype test sections of Fig. 14 were designed on the basis of Eqs. (17) and (18) as diverging sections with a straight taper from $R_o$ to $R_2$ over the length of the test sections (except for the contraction transitions, which were faired into this straight taper). Equation (5) may be used to determine the varying radius of a test section along its length. This equation applies from $X/D_o$ = 0, and that portion of the resulting profile between $X/D_o$ = 0.25 and $X/D_o$ = 2.26 would be used for the diverging test section (the contraction transition would be faired to this profile). If this were done, the radius would not increase linearly with length but would increase at a decreasing rate downstream along

the test section. Computations indicate that the difference in $R/R_o$ between the concave profiles from Eq. (5) and a straight taper decreases with increasing Reynolds number. The maximum difference between the radius of the curve and the radius of the straight taper, both with equal values of $R_o$ and $R_2$, was computed to be 0.0008 in. for the model and 0.003 in. for the prototype at representative Reynolds numbers. These differences are less than the proportionate tolerances for the diameters in the model and equal to those for the prototype (Fig. 3 of reference [4]). Thus a straight taper is considered to be satisfactory.

# A P P E N D I X  C

FIGURES 1 to 15

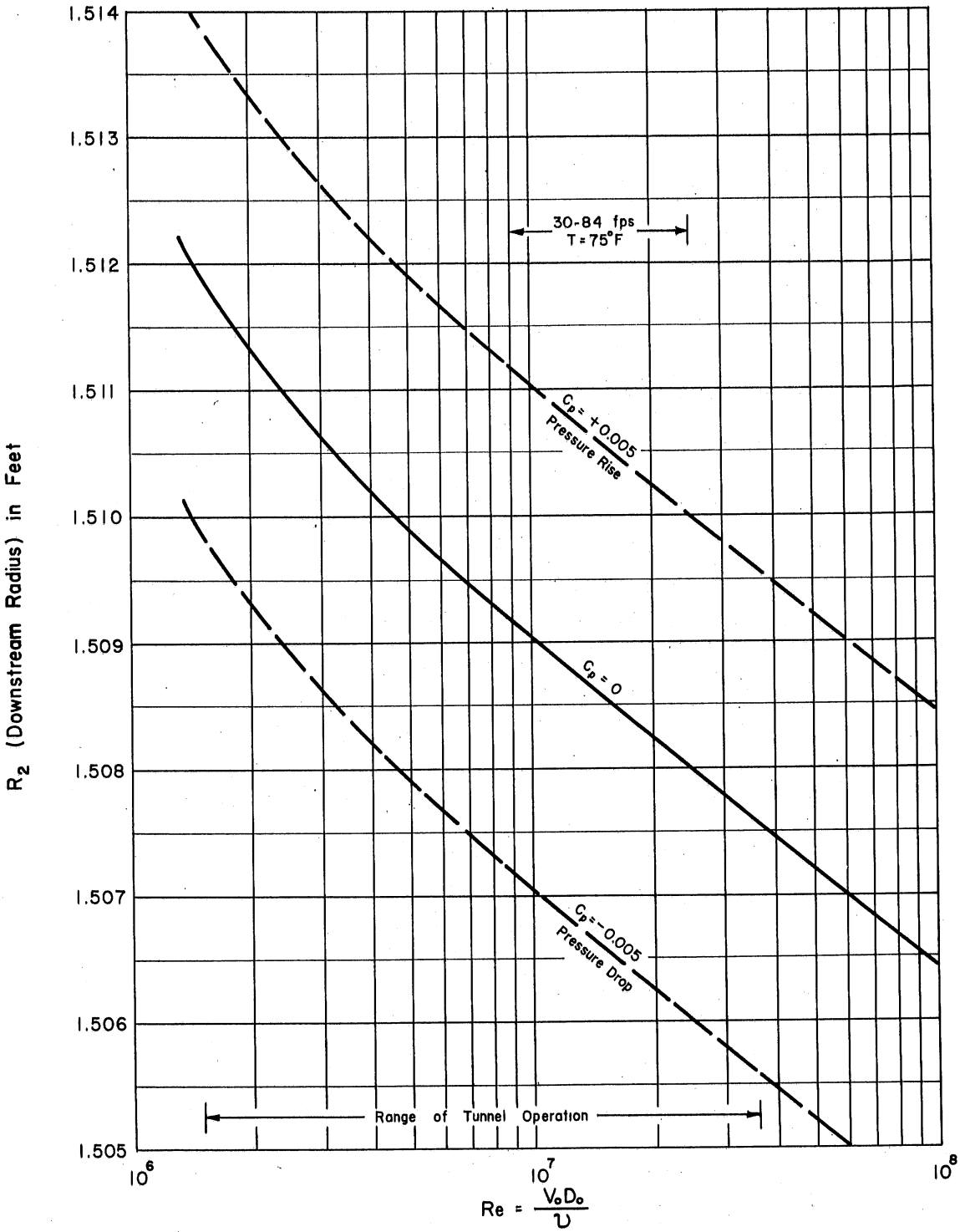


Fig.1 - Estimated Optimum Radius at End of Diverging Closed-Jet Test Section ($\frac{x}{D_o}$ = 2.01) for 36-Inch Water Tunnel

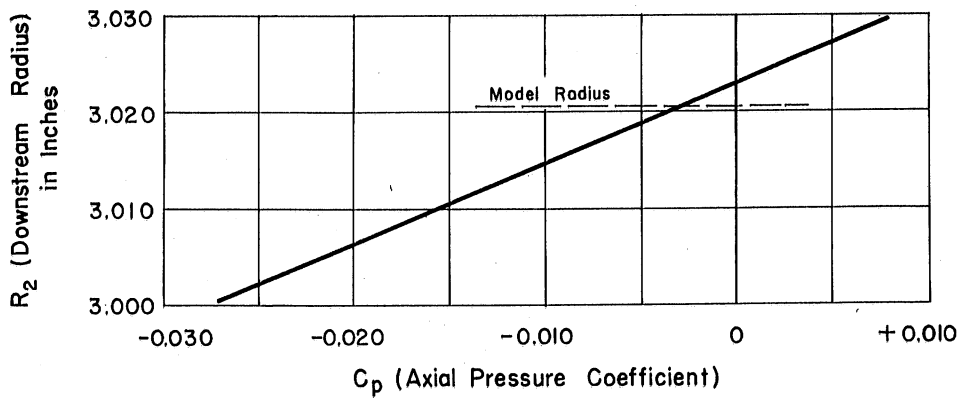


Fig. 2 - Estimated Core Pressure Coefficient for Model Diverging Closed-Jet Test Section

$Re = \frac{V_0 D_0}{\nu} = 2.4 \times 10^6$

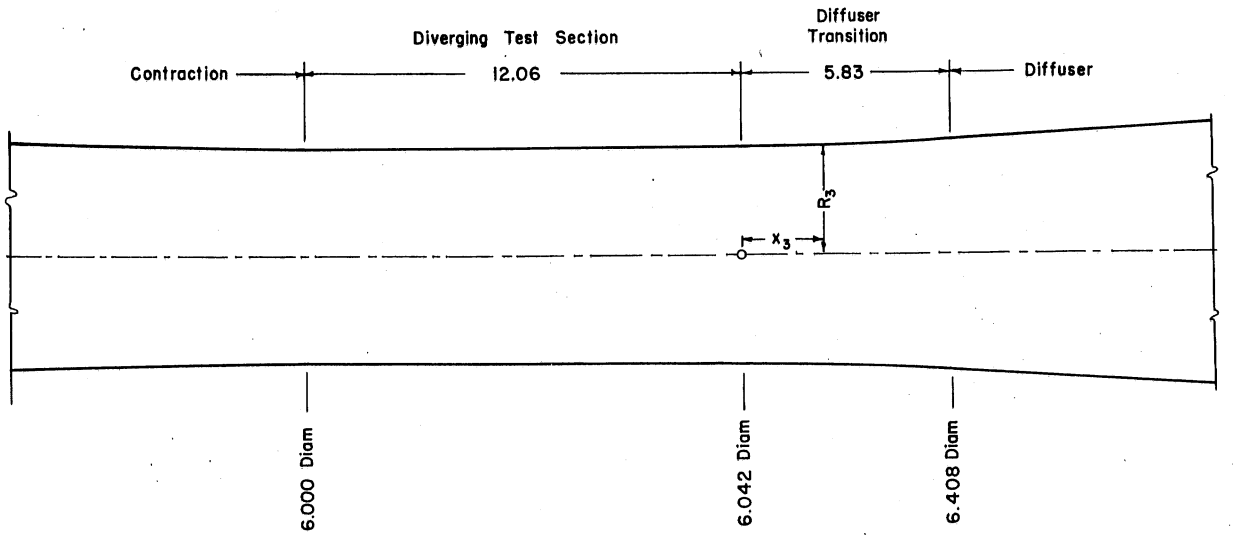


Diffuser Transition Equation: $R_3 = 3.021 + 0.001701 x_3 + 0.00510 x_3^2$

Fig. 3 - Model Diverging Closed-Jet Test Section with Diffuser Transition

Dimensions in inches

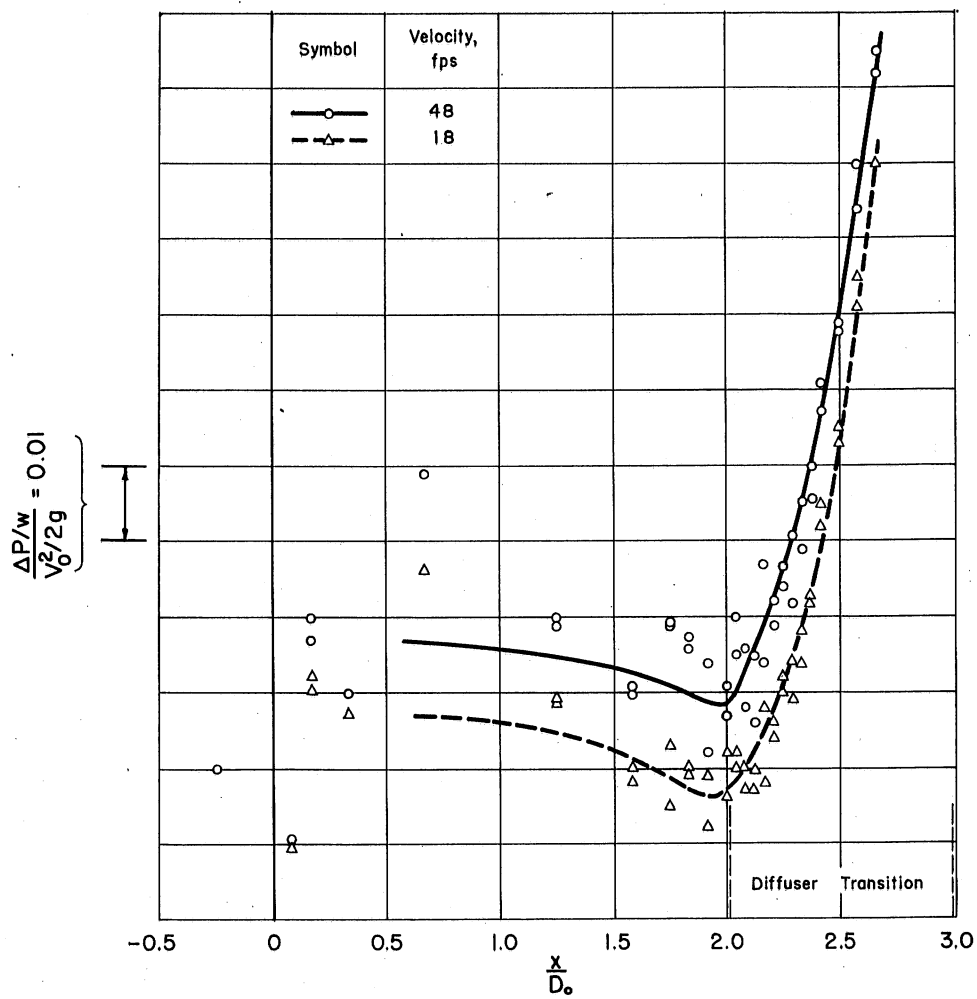


Fig. 4 - Measured Wall Pressure Variation in Diverging Closed-Jet Test Section with Diffuser Transition

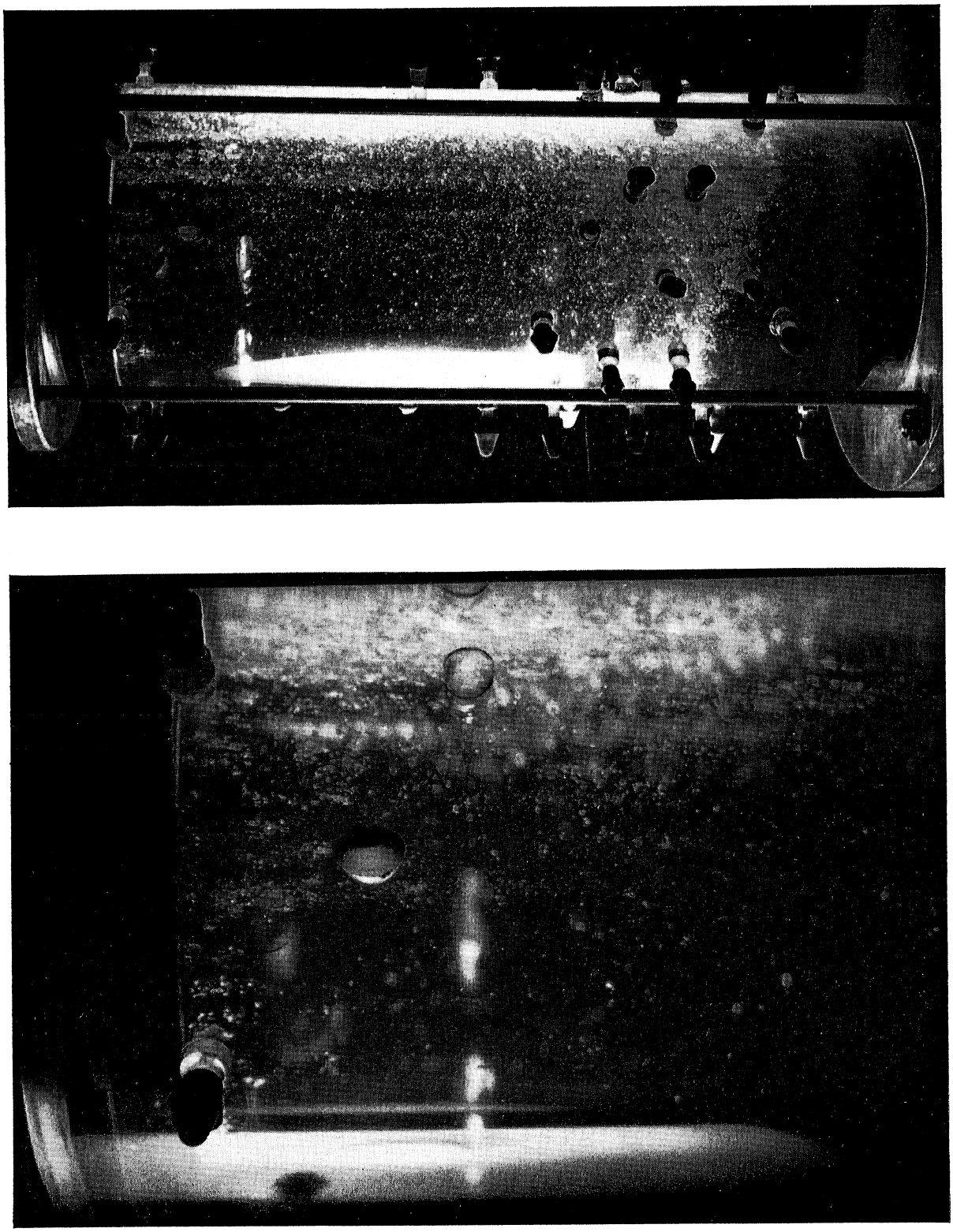

Fig. 5 – Cavitation in Diverging Closed - Jet Test Section with Diffuser Transition

Flow is from left to right

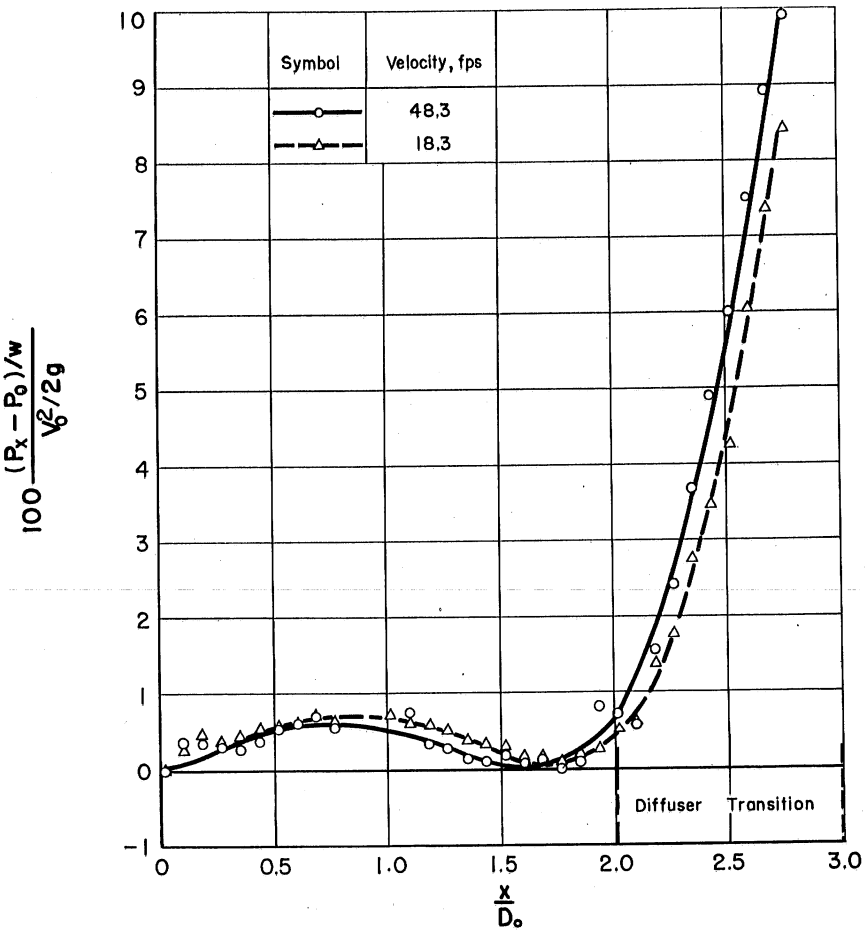


Fig. 6 – Measured Axial Pressure Variation in Diverging Closed-Jet Test Section with Diffuser Transition

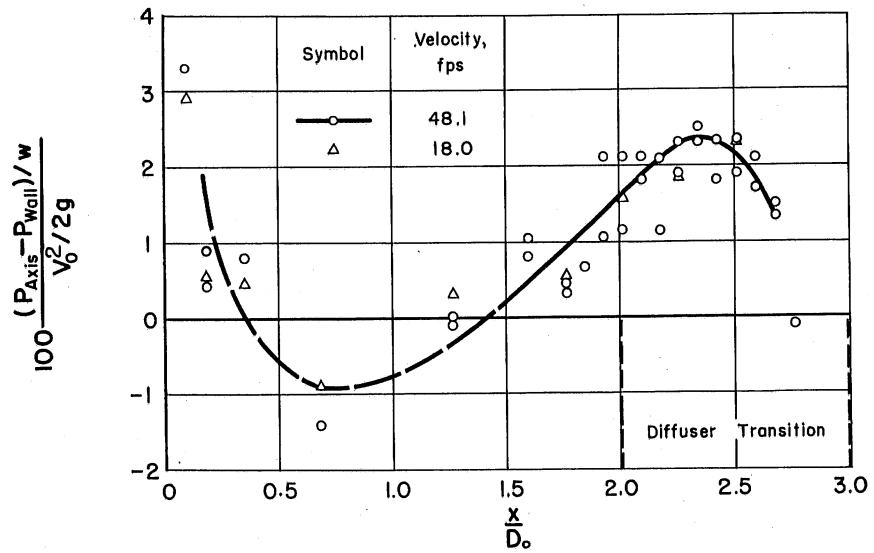


Fig. 7 – Measured Piezometric Pressure Difference Between Axis and Wall in Diverging Closed-Jet Test Section with Diffuser Transition

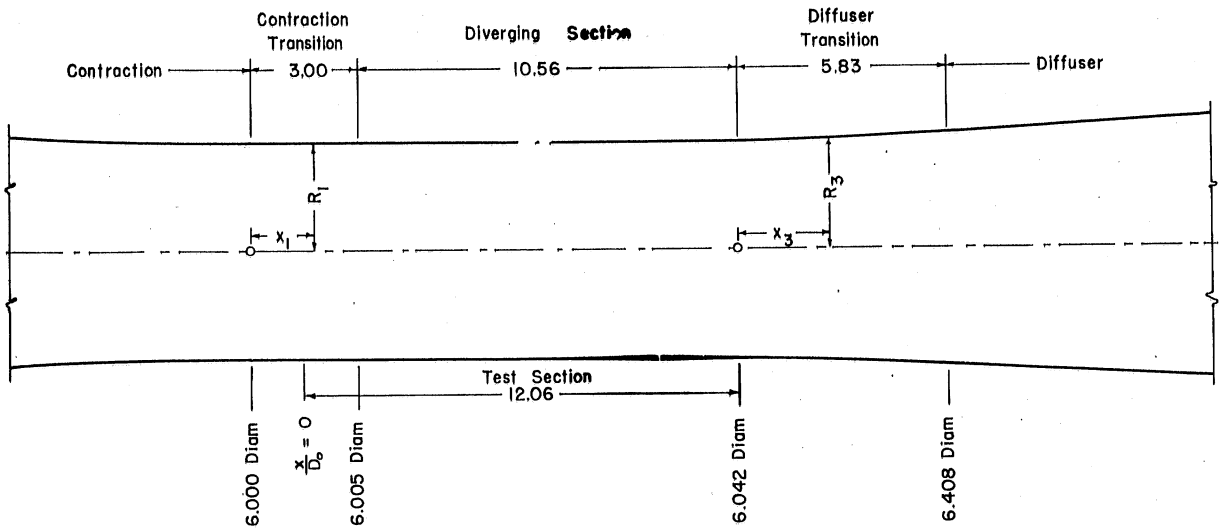


Contraction Transition Equation: $R_1 = 3 + 0.000283\, x_1^2$

Diffuser Transition Equation: $R_3 = 3.021 + 0.001701\, x_3 + 0.00510 x_3^2$

Fig. 8 - Model Diverging Closed-Jet Test Section with Both Contraction and Diffuser Transitions

Dimensions in inches

TABLE I

MODEL TEST-SECTION COORDINATES

(Dimensions are in inches)

| x* | R | x | R | x | R |
|---|---|---|---|---|---|
| -10.00 | 3.321 | 0.00 | 3.0006 | 13.56 | 3.035 |
| - 9.00 | 3.240 | 0.50 | 3.0011 | 14.06 | 3.044 |
| - 8.00 | 3.173 | 1.00 | 3.0018 | 14.56 | 3.057 |
| - 7.00 | 3.118 | 1.50 | 3.0025 | 15.06 | 3.072 |
| - 6.00 | 3.075 | 3.50 | 3.0059 | 15.56 | 3.089 |
| - 5.00 | 3.042 | 5.50 | 3.0093 | 16.06 | 3.109 |
| - 4.00 | 3.020 | 7.50 | 3.0127 | 16.56 | 3.132 |
| - 3.00 | 3.006 | 9.50 | 3.0161 | 17.06 | 3.157 |
| - 2.00 | 3.000 | 11.50 | 3.0195 | 17.56 | 3.184 |
| - 1.50 | 3.000 | 12.06 | 3.021 | 17.89 | 3.204 |
| - 1.00 | 3.0001 | 12.56 | 3.023 | 19.90 | 3.3265 |
| - 0.50 | 3.0003 | 13.06 | 3.027 | | |

*Defined in Fig. 8 and Appendix A.

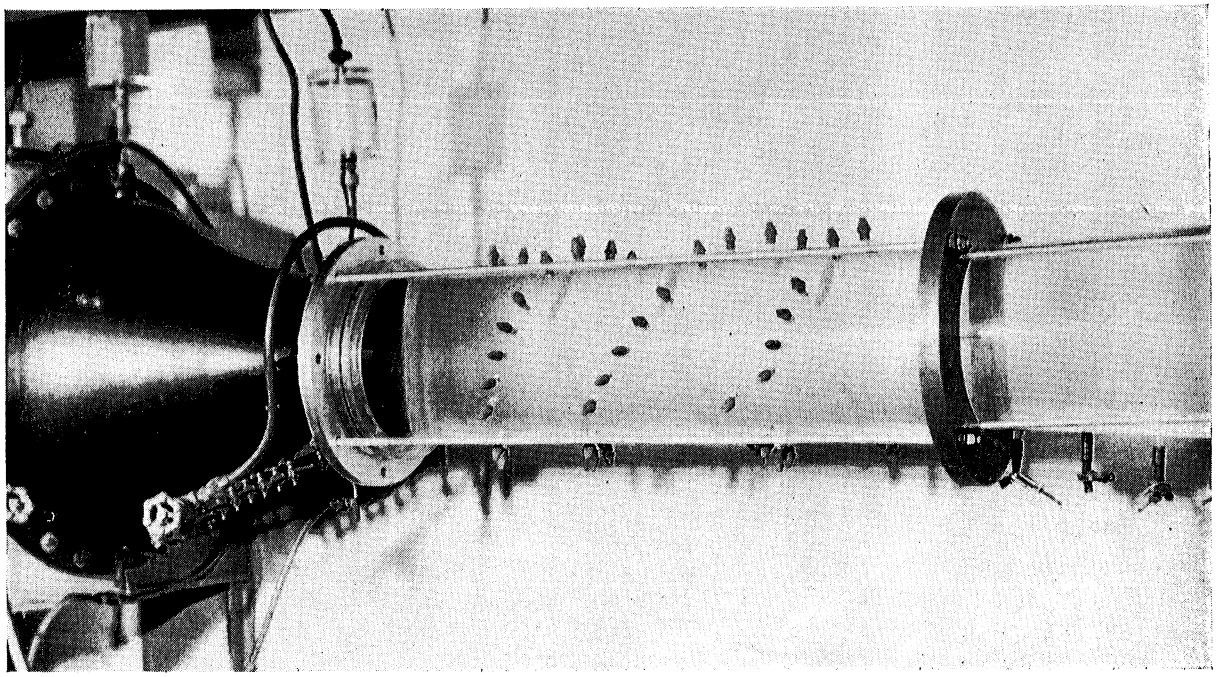

(a) Bare test section

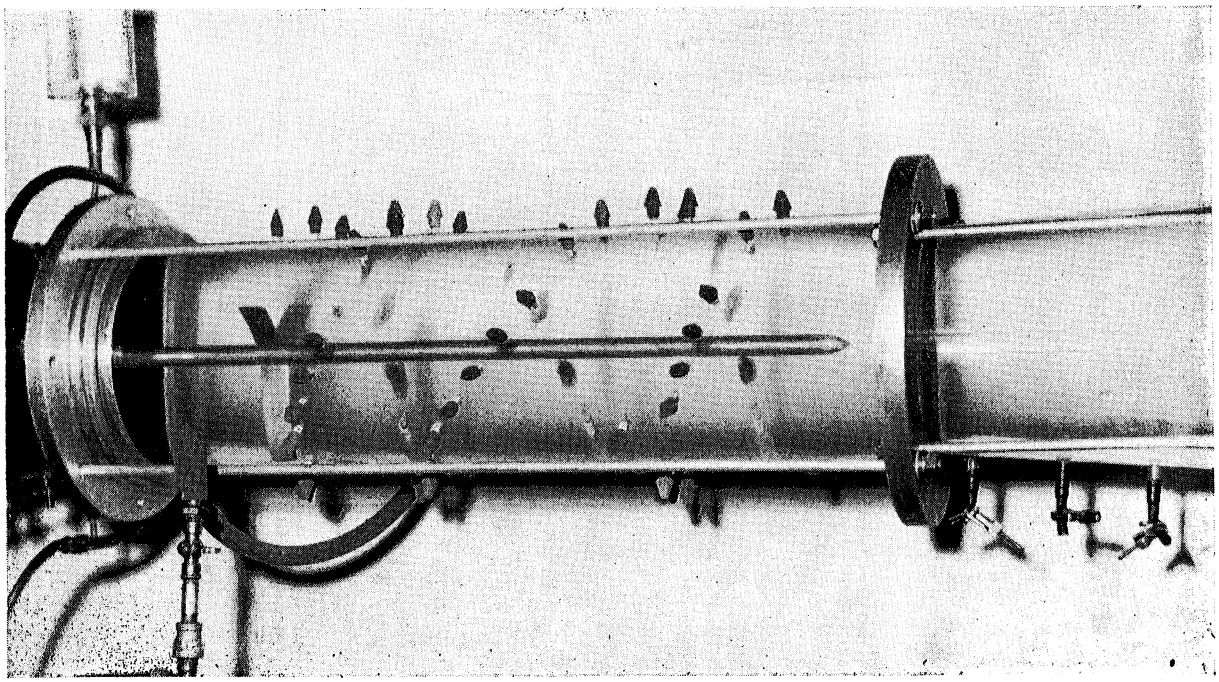

(b) With contraction dynamometer shaft housing

Fig. 9 – Model Diverging Closed-Jet Test Section with both Contraction and Diffuser Transitions

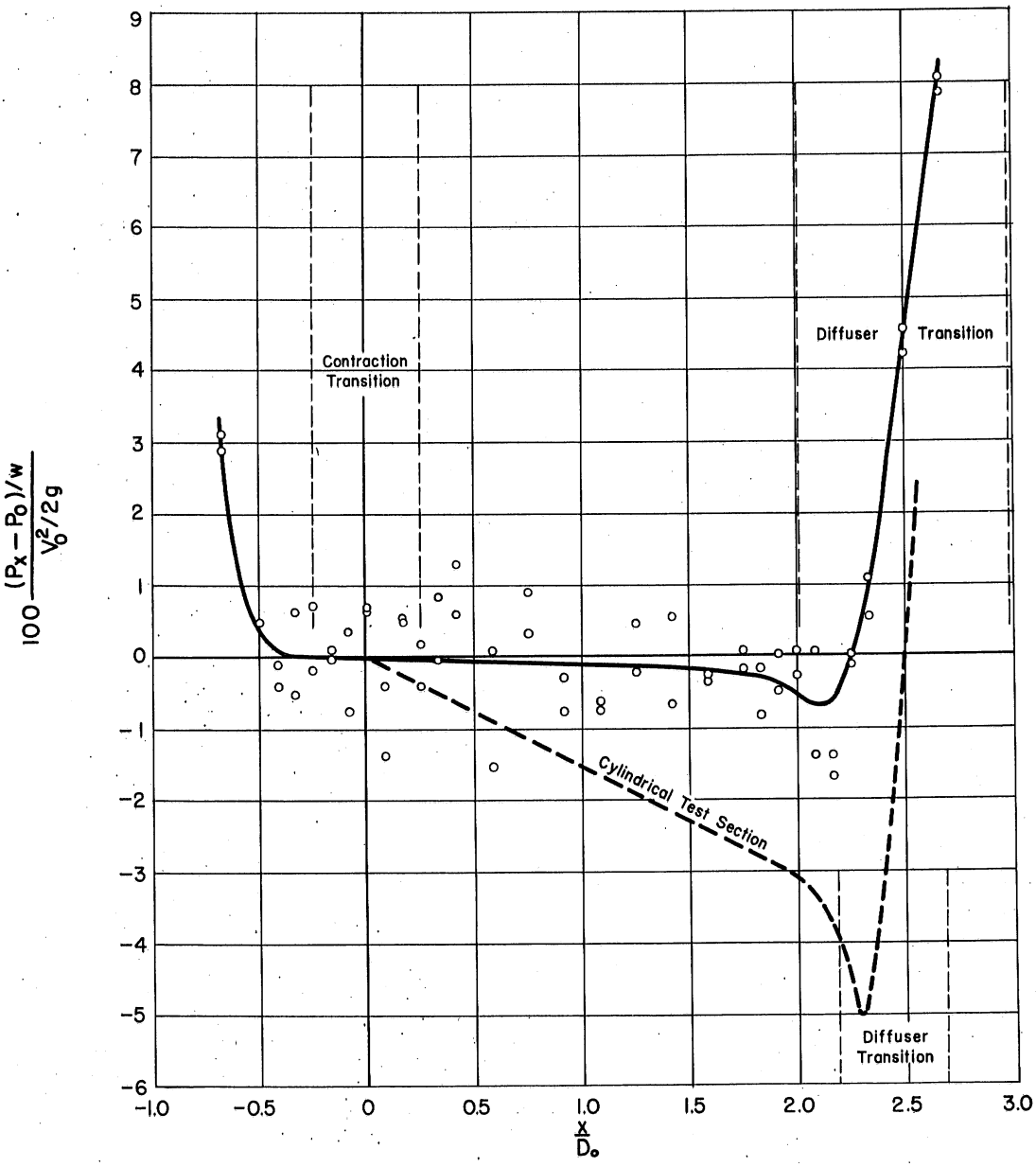


Fig. 10 - Measured Wall Pressure Variation in Diverging Closed-Jet Test Section with Both Contraction and Diffuser Transitions

$V_0$ = 49 fps

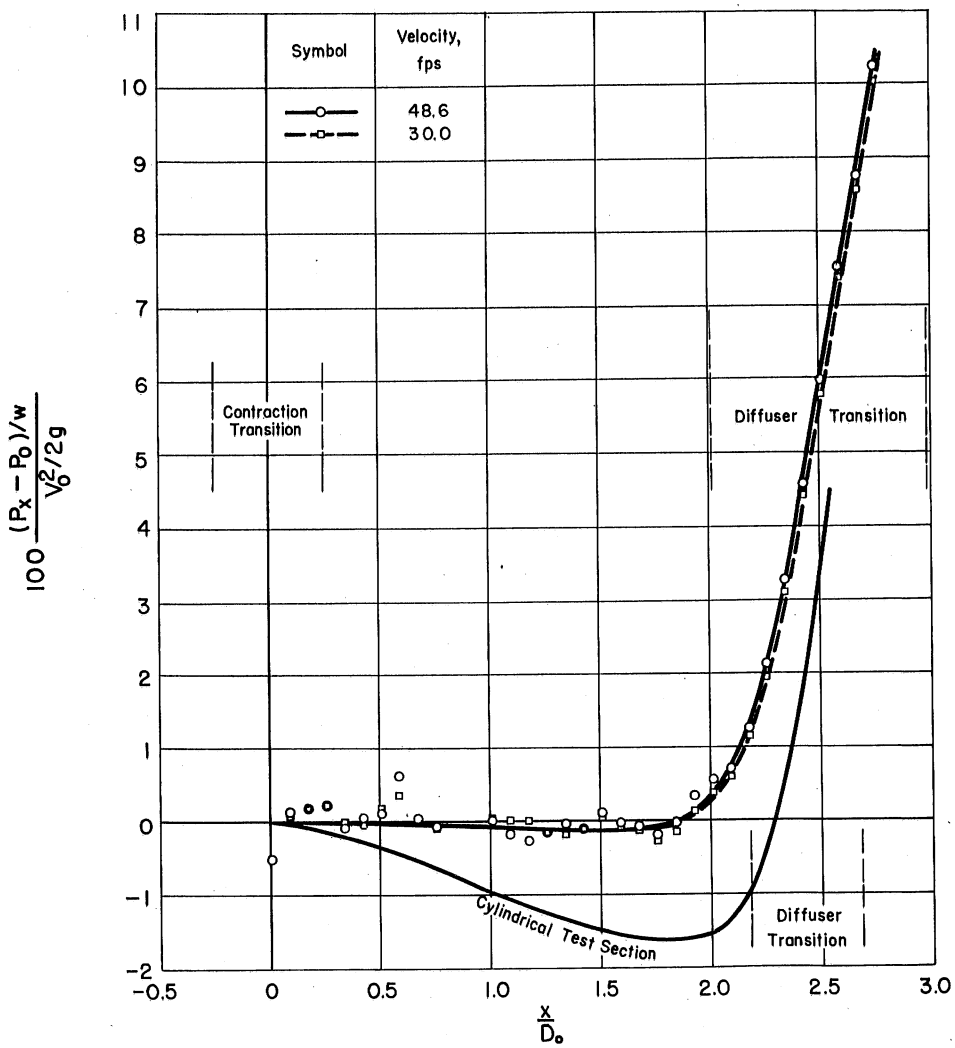


Fig. 11 - Measured Axial Pressure Variation in Diverging Closed - Jet Test Section with Both Contraction and Diffuser Transitions

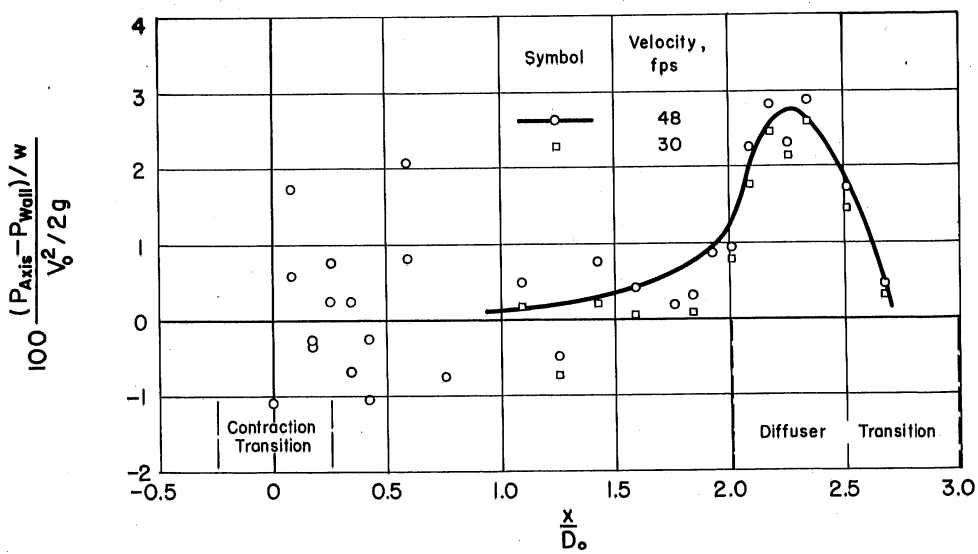


Fig. 12 - Measured Piezometric Pressure Difference Between Axis and Wall in Diverging Closed - Jet Test Section with Both Contraction and Diffuser Transitions

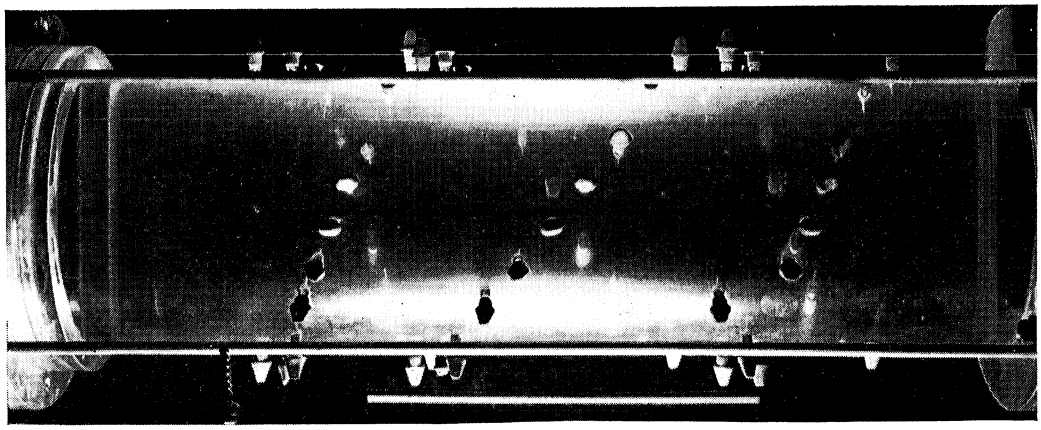

(a) $\sigma_o = 0.06$

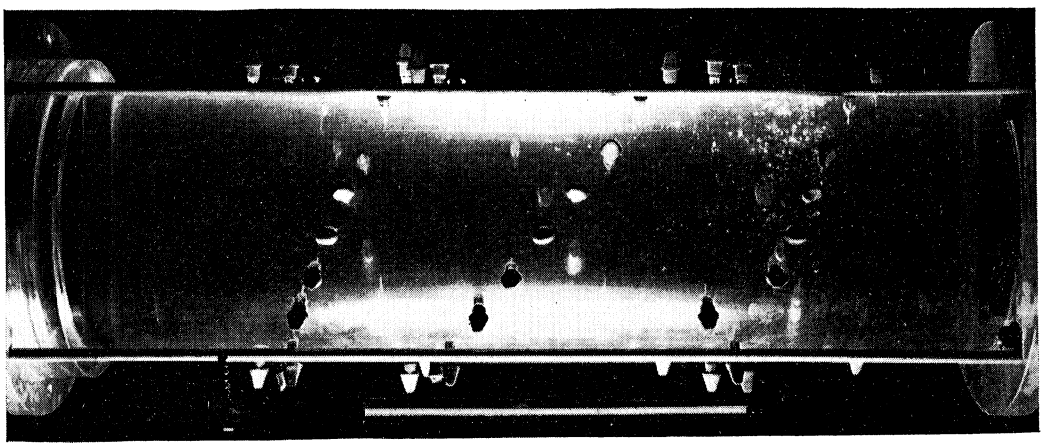

(b) $\sigma_o = 0.022$

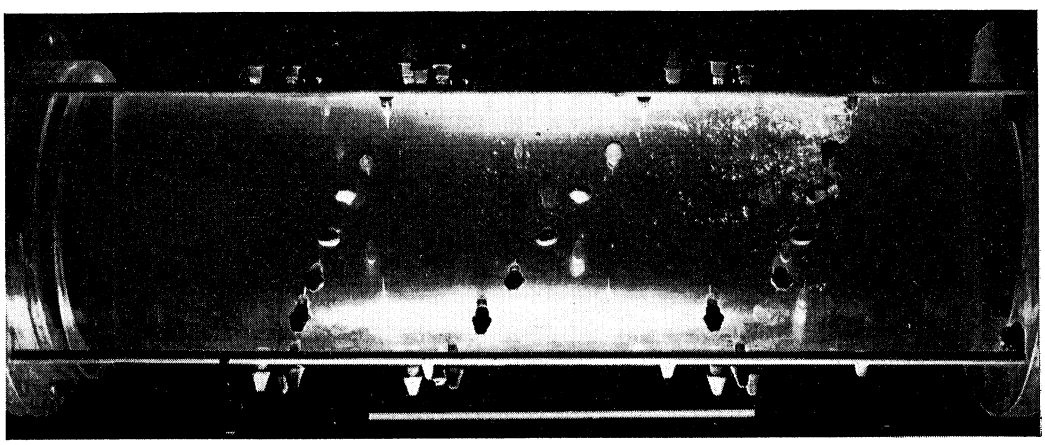

(c) $\sigma_o = 0.014$

Fig. 13 – Various Stages of Cavitation in the Diverging Closed-Jet Test Section with both Contraction and Diffuser Transitions

White lines indicate test section limits
Flow is from left to right

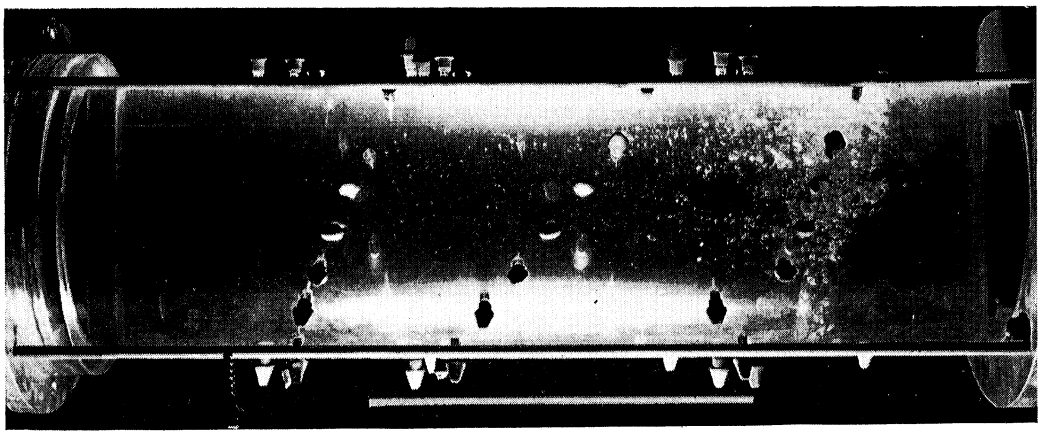

(d) $\sigma_o$ = 0.006

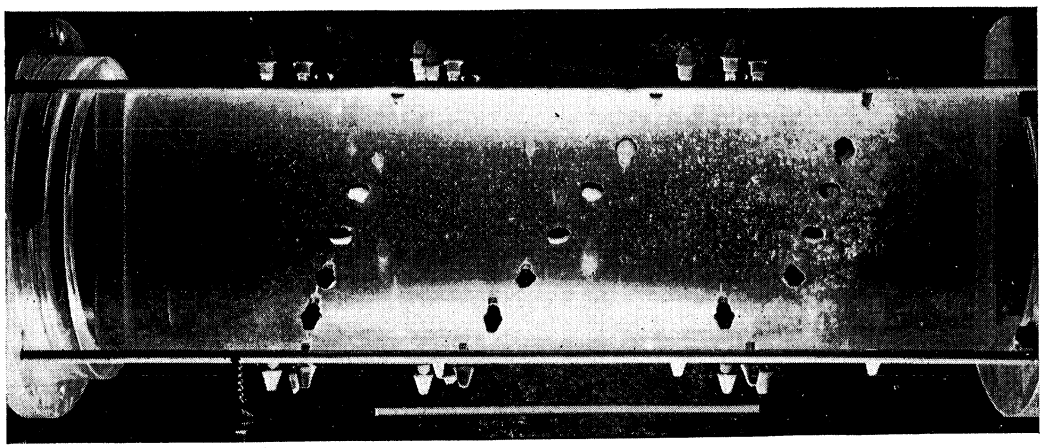

(e) $\sigma_o$ = 0.006

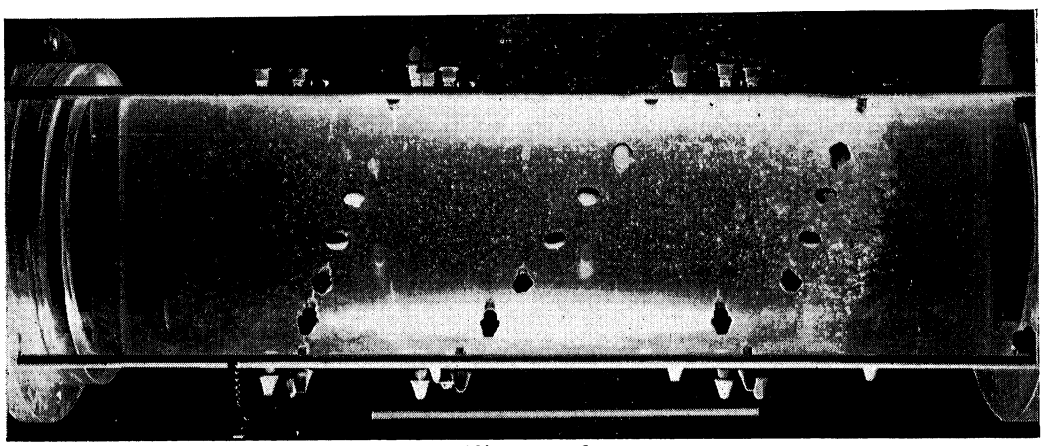

(f) $\sigma_o$ = 0

Fig. 13 – Various Stages of Cavitation in the Diverging Closed-Jet Test Section with both Contraction and Diffuser Transitions

White lines indicate test section limits
Flow is from left to right

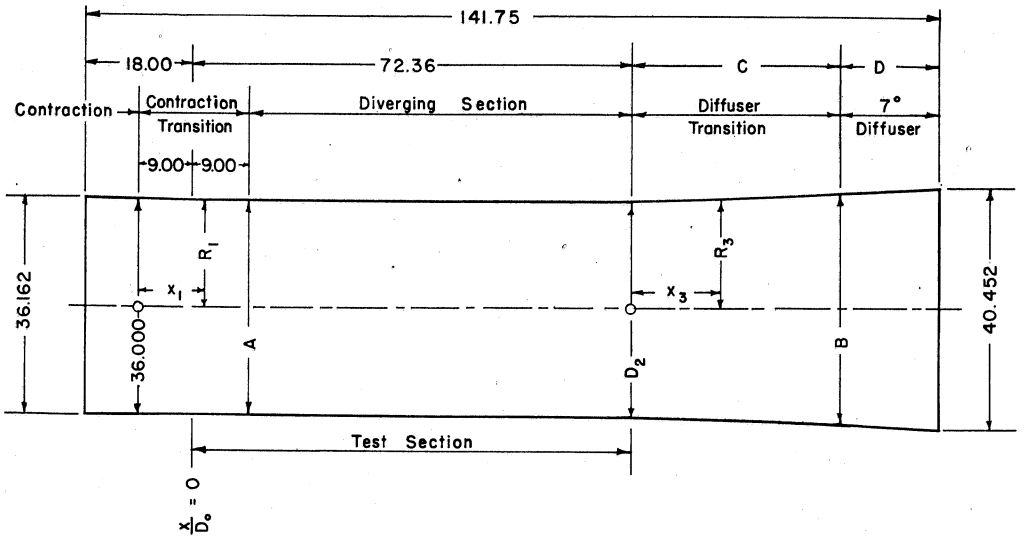


Dimensions in inches

| $R_2$, ft | Contraction Transition Equation | A, in. | Taper, in. per in. | $D_2$, in. | Diffuser Transition Equation | B, in. | C, in. | D, in. |
|---|---|---|---|---|---|---|---|---|
| 1.508 | $\Delta R_1 = .0000369 x_1^2$ | 36.024 | .0013267 | 36.192 | $R_3 = 18.096 + .0013267 x_3 + .000883 x_3^2$ | 38.308 | 33.86 | 17.53 |
| 1.5085 | $\Delta R_1 = .0000392 x_1^2$ | 36.025 | .0014096 | 36.204 | $R_3 = 18.102 + .0014096 x_3 + .000876 x_3^2$ | 38.338 | 34.11 | 17.28 |
| 1.509 | $\Delta R_1 = .0000415 x_1^2$ | 36.027 | .0014925 | 36.216 | $R_3 = 18.108 + .0014925 x_3 + .000868 x_3^2$ | 38.368 | 34.36 | 17.03 |
| 1.5095 | $\Delta R_1 = .0000438 x_1^2$ | 36.028 | .0015755 | 36.228 | $R_3 = 18.114 + .0015755 x_3 + .000861 x_3^2$ | 38.400 | 34.61 | 16.78 |
| 1.51025 | $\Delta R_1 = .0000473 x_1^2$ | 36.031 | .0017013 | 36.246 | $R_3 = 18.123 + .0017013 x_3 + .000850 x_3^2$ | 38.446 | 34.98 | 16.41 |

$R_1 = 18.000 + \Delta R_1$

Fig. 14 – Profiles for a Constant - Pressure Diverging Closed - Jet Test Section for a 36-Inch Water Tunnel

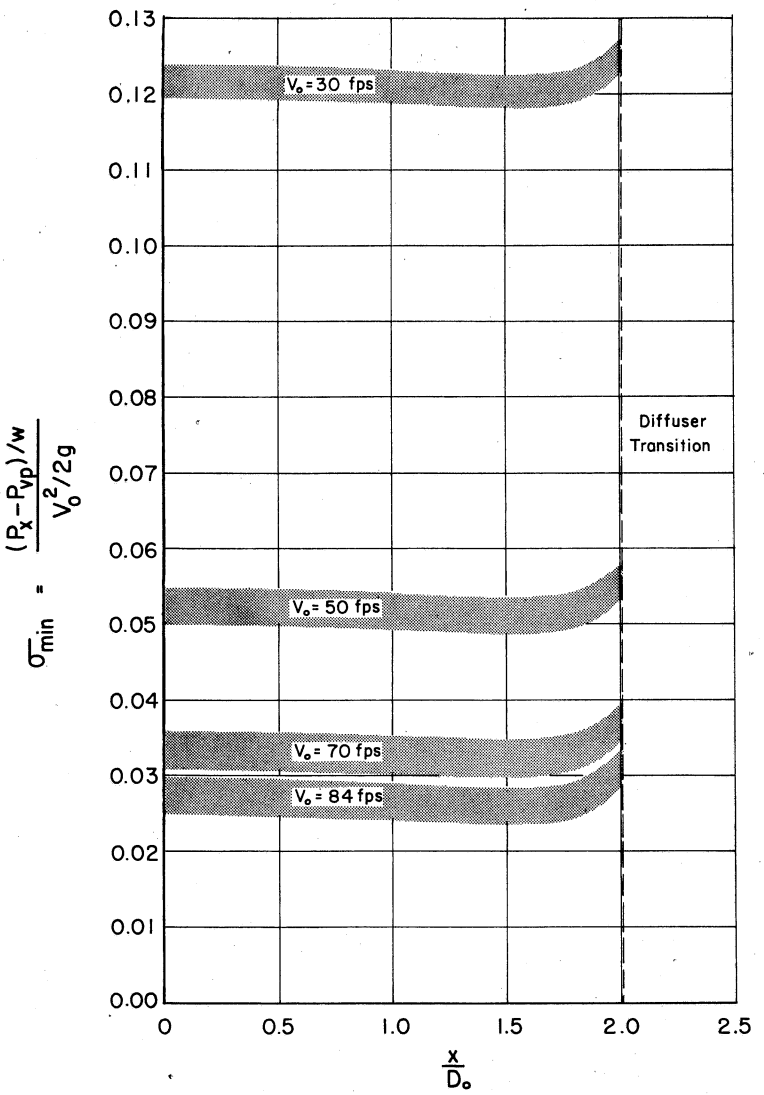


Fig.15 - Estimated Minimum Cavitation Index Along Axis of Diverging Closed-Jet Test Section of 36-Inch Water Tunnel